

Bicritical and tricritical phenomena in uniaxial ferromagnets

M. R. H. Khajepour,* Yung-Li Wang,[†] and Robert A. Kromhout*

Department of Physics, The Florida State University, Tallahassee, Florida 32306

(Received 24 March 1975)

The phase diagrams of a spin-1 uniaxial ferromagnetic model with both exchange anisotropy and single-ion anisotropy (D) are studied in the mean-field approximation. In the absence of an external magnetic field a bicritical point (BCP) is found in the (D, T) plane for the transverse (K) to parallel (J) coupling ratio $K/J > 0.462$. As the exchange anisotropy is decreased the BCP moves towards the temperature axis. In the limit of the isotropic exchange the BCP is located on the T axis. In the presence of a field along the parallel (transverse) direction two symmetric lines of tricritical points (TCP) are generated in the $(D, H_2(H_1), T)$ space. These lines meet at the BCP. For a significantly wide range of D/J and K/J values TCP prevails in the $(H_2(H_1), T)$ plane. Application of a transverse (parallel) field generates the wing coexistence surfaces. The whole thermodynamic space is experimentally accessible. Outside the above ranges, one may still have a TCP in the (H_1, T) plane, but not in the (H_2, T) phase diagram. Some special features of the (H_2, T) phase diagram are also discussed.

I. INTRODUCTION

The study of the systems exhibiting multicritical phenomena has recently attracted much attention. While some types of multicritical behavior have been known to exist for many years¹ the recent intense interest in the subject reflects two great advancements: a fairly basic and thorough understanding of ordinary critical phenomena through the hypothesis of thermodynamic scaling and the renormalization-group approach, and the development of high-precision techniques and ingenious designs for measurements, which make the critical region amenable to experimental scrutiny. The study of the multicritical phenomena also allows us to examine the validity of the existing concepts of homogeneity and universality or the possibility of their extension.

By now quite a few physical systems are known to exhibit tricriticality.² The existence of bicritical points (BCP) in the uniaxially anisotropic antiferromagnets in a uniform magnetic field³ and in the ferromagnetic-ferroelectric systems⁴ has been known for some time, although the implications of the bicritical singularities have not been appreciated until quite recently.⁵ Tetracritical phenomena are newcomers on the scene. Their existence has been reported in certain magnetic alloys⁶ and in mixed crystals.⁷

A multicritical point is characterized by the existence of several phase transitions (which may be of different natures) in its vicinity. Near a tricritical point the interplay is between first-order and second-order phase transitions, and a single order parameter is sufficient to describe both transitions. In systems exhibiting bi- and tetracritical phenomena we have more than one kind of ordered state. The phase transitions are from ordered states to paramagnetic phase as well as between the ordered phases. Therefore the behavior of these systems depends upon the competition between the

two order parameters; e.g., the parallel and the transverse (in flop phase) sublattice magnetizations in the uniaxial antiferromagnets in a field,³ the polarization and the magnetization in ferromagnetic-ferroelectric,⁴ the crystalline and superfluid (diagonal and off-diagonal long-range orders) in ⁴He,⁸ and two types of magnetic ordering in the magnetic mixed crystals.^{6,7} Theories based on the mean-field approximation^{3,8} and the phenomenological Landau-type expansions^{4,8,9} have been applied to the above systems. Liu and Fisher⁸ and Bruce and Aharony¹⁰ have given a succinct Landau-type theory of the bi- and tetracritical points. A similar theory for tricritical systems is developed by Bausch.¹¹ In this rather general and qualitatively correct context, bi-, tri-, and tetracritical points are defined as the points where two, three, and four critical lines meet, respectively. While the coexistence of two "pure" phases (defined by the two order parameters) along a line (flop line) is necessary to have a BCP, at temperatures below a tetracritical point an intermediate or "mixed" phase lies between the two "pure" phases. Another approach¹² indicates that this picture may not be complete if the full thermodynamic field space is considered.

Fisher and Nelson⁵ have postulated a scaling hypothesis for BCP of a uniaxially anisotropic antiferromagnet in a field. A similar homogeneity hypothesis was applied to a model by Chang *et al.*¹² and Harbus *et al.*¹³ The renormalization-group technique¹⁴ applied to a classical n -vector model of a uniaxial antiferromagnet in a field, confirms the scaling hypothesis, and leads to an important consequence¹⁵: for $n \leq n^*(d)$ [$n^*(d) > 3$ for $d = 3$] the bicritical exponents are the same as those of a fully isotropic Heisenberg system.

The application of the scaling hypothesis near a BCP has two important consequences⁵: (i) additional scaling laws hold among the bicritical exponents, and (ii) the critical lines and the flop line have a

common tangent at BCP.

In the models discussed in Refs. 5, 10, and 13, the ordering fields are either physically fictitious fields or experimentally uncontrollable.¹⁶ Therefore one cannot investigate the vicinity of the BCP in all directions experimentally. The features in the vicinity of a BCP are of great interest. For example, it is shown by Chang *et al.*¹² that four tricritical lines meet at a BCP in a generalized metamagnetic model. The ordering fields to generate these lines in all the above models are the staggered fields.

In this paper we discuss an anisotropic uniaxial ferromagnetic model which exhibits, in addition to the ordinary critical phenomena, bicriticality at $\vec{H}=0$ and tricriticality in a finite field. The Hamiltonian contains a single-ion term of the form $D(S_z)^2$. The exchange interaction is also assumed to be anisotropic. A magnetic field along either the parallel or the transverse direction generates two tricritical lines which terminate at the BCP. Consequently, in a region near the BCP one expects a variety of critical (either Ising-like or xy -like), bicritical, and tricritical behaviors, as well as the crossovers between these behaviors.

Another interesting feature of the model is that when the anisotropy D is treated as a constant, ($H_z, H_\perp=0, T$) and ($H_z=0, H_\perp, T$) phase diagrams exhibit a tricritical point (TCP) for a wide range of the values of the parameters of the system. Here one has a situation where the TCP and the wings are all within an experimentally accessible and controllable thermodynamic field space. This same feature is shown in the Blume-Capel model in a transverse field (which is a special case of our more general model) and has been discussed by the authors elsewhere.¹⁷

In order to have a general picture of the phase diagrams, we have carried out an investigation of this model in the mean-field approximation (MFA). The model Hamiltonian is discussed in Sec. II. We have obtained the zero-field partition function as a double expansion in the order parameters. The zero-field phase diagrams in the whole range of the transverse coupling $K > 0$ is obtained in Sec. III. The range of values of K where the phase diagram contains a BCP is found. The study of the system in a finite magnetic field is the subject of Sec. IV. The behaviors of the system in a parallel and a transverse field are treated separately, and the corresponding phase diagrams are worked out. The ranges of the parameters D and positive K where tricritical behavior exists are found. Finally in Sec. V the main points of the work are summarized.

II. MODEL HAMILTONIAN

We consider a spin-1 uniaxial ferromagnet with an anisotropic exchange interaction and a single-

ion anisotropy

$$\mathcal{H} = - \sum_{\langle ij \rangle} J_{ij} S_z(i) S_z(j) - \sum_{\langle ij \rangle} K_{ij} \vec{S}_\perp(i) \cdot \vec{S}_\perp(j) + \Delta \sum_i [S_z(i)]^2 - \mu \vec{H} \cdot \sum_i \vec{S}(i), \quad (2.1)$$

where J and K are assumed positive. The transverse coupling provides the possibility for the system to order in the basal plane perpendicular to the z axis for certain ranges of temperature and anisotropy. In the mean-field approximation (MFA) the Hamiltonian (2.1) can be written

$$\mathcal{H}_m = -2\langle S_z \rangle S_z - 2K\langle S_\perp \rangle S_\perp + D(S_z)^2 - \vec{h} \cdot \vec{S} + \langle S_z \rangle^2 + K\langle S_\perp \rangle^2, \quad (2.2)$$

where $K = K(0)/J(0)$, $\vec{h} = \mu \vec{H}/J(0)$, $D = \Delta/J(0)$, $J(0) = \sum_j J_{ij}$, $K(0) = \sum_j K_{ij}$, and energies are measured in units of $J(0)$.

It should be noted that while the basal plane is isotropic we have chosen a direction for the ordering and have labeled it with the perpendicular sign; $\langle S_\perp \rangle$ is the component of $\langle \vec{S} \rangle$ on the basal plane.

One can write Eq. (2.2) in an even simpler form

$$\mathcal{H}_m = D(S_z)^2 - \alpha_z S_z - \alpha_\perp S_\perp + \epsilon_0, \quad (2.3)$$

where

$$\begin{aligned} \alpha_z &= h_z + 2\langle S_z \rangle, \\ \alpha_\perp &= h_\perp + 2\langle S_\perp \rangle, \\ \epsilon_0 &= \langle S_z \rangle^2 + K\langle S_\perp \rangle^2. \end{aligned} \quad (2.4)$$

The energy eigenvalues of \mathcal{H}_m are the roots of the secular equation

$$\lambda_k^3 - 2D\lambda_k^2 + (D^2 - \alpha_z^2 - \alpha_\perp^2)\lambda_k + D\alpha_\perp^2 = 0. \quad (2.5)$$

Equation (2.5) can be solved by standard methods to yield the result

$$\begin{aligned} E_k &= \lambda_k + \epsilon_0 \\ &= \frac{2}{3}D + \frac{2}{3}(D^2 + 3\alpha_z^2 + 3\alpha_\perp^2)^{1/2} \cos[\phi + \frac{2}{3}\pi(k-1)] + \epsilon_0, \end{aligned} \quad (2.6)$$

where $k=1, 2, 3$ and,

$$\cos(3\phi) = -\frac{1}{2} \frac{2D^3 - 18(\alpha_z^2 + \alpha_\perp^2)D + 27\alpha_\perp^2 D}{(D^2 + 3\alpha_z^2 + 3\alpha_\perp^2)^{3/2}}. \quad (2.7)$$

Equations (2.6) and (2.7) are used for numerical calculations. For the special cases of $H_z=0$ (or $H_\perp=0$) a simple expansion in $\langle S_z \rangle$ (or $\langle S_\perp \rangle$) can be easily obtained from Eq. (2.5) in the vicinity of a second-order phase transition. In general one can use Eq. (2.6) to find a set of self-consistent equations for the parallel and the transverse magnetizations.

In the limit of zero external field a perturbation

expansion of energy eigenvalues about $\langle S_1 \rangle = 0$ (or $\langle S_z \rangle = 0$) is a convenient approach to discuss the second-order phase transitions. To do this one assumes that $\langle S_z \rangle$ (or $\langle S_1 \rangle$) is finite:

$$E_+ = \epsilon_+ + \frac{D^2}{2\epsilon_+} \lambda^2 - \frac{\epsilon_- D^4}{16\langle S_z \rangle \epsilon_+^3} \lambda^4 + \dots + \epsilon_0, \quad (2.8a)$$

$$E_- = \epsilon_- + \frac{D^2}{2\epsilon_-} \lambda^2 + \frac{\epsilon_+ D^4}{16\langle S_z \rangle \epsilon_-^3} \lambda^4 + \dots + \epsilon_0, \quad (2.8b)$$

$$E_0 = -\frac{D^2}{2} \left(\frac{1}{\epsilon_+} + \frac{1}{\epsilon_-} \right) \lambda^2 \\ \times \frac{D^4}{4} \left(\frac{1}{\epsilon_+} + \frac{1}{\epsilon_-} \right) \left(\frac{1}{\epsilon_+^2} + \frac{1}{\epsilon_-^2} \right) \lambda^4 + \dots + \epsilon_0, \quad (2.8c)$$

where

$$\epsilon_{\pm} = D(1 \mp \eta), \\ \eta = \frac{2\langle S_z \rangle}{D}, \\ \lambda = \frac{2K\langle S_1 \rangle}{D}. \quad (2.9)$$

Although it may appear that Eqs. (2.8a) and (2.8b) blow up as $\langle S_z \rangle \rightarrow 0$, in the calculation of the partition function one can show that all divergent terms from the two energy levels cancel each other, and so the free energy is actually an analytic function of both $\langle S_z \rangle$ and $\langle S_1 \rangle$. The final result can be written as a double expansion of the partition function Z , for small values of $\langle S_z \rangle$ and $\langle S_1 \rangle$.

$$Z = \sum_i e^{-\beta E_i} \\ = e^{-\beta \epsilon_0} (Z_0 + Z_1 \lambda^2 + Z_2 \eta^2 + Z_3 \eta^2 \lambda^2 + Z_4 \eta^4 + Z_5 \lambda^4), \quad (2.10)$$

where

$$Z_0(\gamma) = 1 + 2e^{-\gamma}, \quad (2.11a)$$

$$Z_1(\gamma) = \gamma(1 - e^{-\gamma}), \quad (2.11b)$$

$$Z_2(\gamma) = \gamma^2 e^{-\gamma}, \quad (2.11c)$$

$$Z_3(\gamma) = \gamma [1 - e^{-\gamma} (1 + \gamma + \frac{1}{2} \gamma^2)], \quad (2.11d)$$

$$Z_4(\gamma) = \frac{1}{12} \gamma^4 e^{-\gamma}, \quad (2.11e)$$

$$Z_5(\gamma) = \gamma [\frac{1}{2} \gamma - 1 + e^{-\gamma} (1 + \frac{1}{2} \gamma)], \quad (2.11f)$$

$$\gamma = \beta D, \quad \beta = \frac{1}{t} = \frac{J(0)}{kT}. \quad (2.12)$$

One gets the same final results if one assumes $\langle S_1 \rangle$ to be finite and expands the energy eigenvalues in $\langle S_z \rangle$.

In a field parallel to the z axis, $\langle S_1 \rangle$ is the appropriate order parameter. A simple classical calculation at $t=0$ shows that two phases are possible: (i) a phase with moments parallel to the applied field, and (ii) a canted phase in which the z component vanishes when h_z tends to zero. The perturbation calculation corresponding to this case has

been worked out in Ref. 18. We refer the reader to that paper for the details of calculation.

When a transverse field is applied, again two phases are possible, a canted phase and a phase with moments only in the basal plane. In this case, $\langle S_z \rangle$ is the appropriate order parameter, and one expands the partition function in powers of $\langle S_z \rangle$.

III. PHASE TRANSITIONS IN ZERO EXTERNAL FIELD

Using Eq. (2.10), one can write the Landau free energy

$$F = -(1/\beta) \ln Z, \quad (3.1)$$

$$f = f_0 + f_1 \lambda^2 + f_2 \eta^2 + f_3 \eta^2 \lambda^2 + f_4 \eta^4 + f_5 \lambda^4 + \dots, \quad (3.2)$$

where

$$f = \beta F, \quad f_0 = \beta F_0 = -\ln Z_0, \quad (3.3a)$$

$$f_1 = \frac{\gamma D}{4K} - \frac{Z_1}{Z_0}, \quad (3.3b)$$

$$f_2 = \frac{\gamma D}{4} - \frac{Z_2}{Z_0}, \quad (3.3c)$$

$$f_3 = \frac{1}{Z_0} \left(\frac{Z_1 Z_2}{Z_0} - Z_3 \right), \quad (3.3d)$$

$$f_4 = \frac{1}{Z_0} \left(\frac{Z_2^2}{2Z_0} - Z_4 \right), \quad (3.3e)$$

$$f_5 = \frac{1}{Z_0} \left(\frac{Z_1^2}{2Z_0} - Z_5 \right). \quad (3.3f)$$

The coefficients f_3 , f_4 , and f_5 are functions of γ only. The dependence of f on K is only through the coefficient f_1 . One should note that knowledge of sixth-order terms is needed only for checking the stability at TCP.

The Landau free energies of the form (3.2) have been discussed by Liu and Fisher,⁸ Wegner,⁹ and more recently by Bruce and Aharony.¹⁰ We just mention the results for the case when $f_3 > 0$, which is of relevance to our model. The continuous transition from the phase with $\eta \neq 0$, $\lambda = 0$ (Z phase) to the paramagnetic phase (P) happens when $f_2 = 0$; f_1 , $f_4 > 0$,

$$f_2 = \frac{1}{4} \gamma [D - D_c(\gamma)] = \frac{1}{4} \gamma^2 [t - t_c(\gamma)], \quad (3.4)$$

where

$$D_c(\gamma) = 4Z_2/\gamma Z_0, \quad t_c(\gamma) = 4Z_2/\gamma^2 Z_0, \quad (3.5)$$

i. e., at $D = D_c(\gamma)$ [or $t = t_c(\gamma)$].

The transition from the $\lambda \neq 0$, $\eta = 0$ phase (T phase) to the paramagnetic phase occurs at $f_1 = 0$, f_2 , $f_5 > 0$,

$$f_1 = \frac{1}{4} \gamma [d - d_c(\gamma)] = (\gamma^2/4K) [t - t'_c(\gamma)], \quad (3.6)$$

where

$$d = D/K \quad (3.7a)$$

and

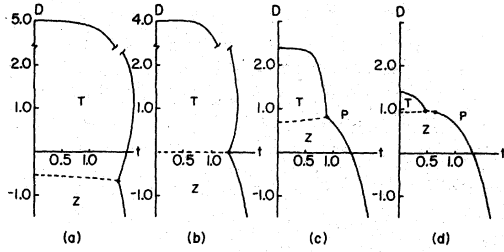


FIG. 1. Phase diagrams in (D, t) plane for different K values. The BCP is the intersection of the two critical lines (solid) and flop line (dashed). T and Z designate the phases with orderings in the basal plane and along the z axis, respectively. (a) $K=1.25$, (b) $K=1.00$, (c) $K=0.6$, and (d) $K=0.35$.

$$d_c = \frac{4}{\gamma} \frac{Z_1}{Z_0}, \quad t'_c = \frac{4K}{\gamma^2} \frac{Z_1}{Z_0}. \quad (3.7b)$$

The paramagnetic phase is stable against a transition to the above phases when both f_1 and f_2 are positive. In general, a phase with both $\lambda \neq 0$ and $\eta \neq 0$ would be stable⁸ only if

$$g = (\frac{1}{2}f_3)^2 - f_4f_5 < 0. \quad (3.8)$$

Numerical calculation shows that for all values of the parameter $\gamma > 0$, $g > 0$. Consequently, the canted phase ($\bar{h}=0$) is never stable for our model. The transition between $\eta \neq 0$, $\lambda=0$ phase (Z phase) and $\lambda \neq 0$, $\eta=0$ phase (T phase) is of first order (flop transition) and occurs whenever

$$f_1 = (f_5/f_4)^{1/2} f_2 < 0 \quad (3.9)$$

provided f_5 and f_4 are positive. One can easily show that f_5 is always non-negative (i.e., a $T \rightarrow P$ phase transition is always of second order) while f_4 changes sign at $D=0.924$ and $t=0.67$, (which is the Blume-Capel TCP). Equation (3.9), is the equation of the flop line close to the point where it meets with the two second-order transition lines. When $f_4 > 0$ the two critical lines $f_1=0$ and $f_2=0$ and the flop line meet at the bicritical point (BCP) (D_b, t_b) . When $f_4 < 0$ the phase diagram ceases to contain a BCP. This happens when $K < 0.462$. At $K=0.462$, $f_1=f_2=f_4=0$. The possible phase diagrams in the $D-t$ plane are shown in Fig. 1. One can distinguish the following cases:

$K > 1$. In this case the flop line is below the t axis, and is bent slightly downwards [Fig. 1(a)].

$K=1$. The flop line is along the $D=0$ axis, and BCP is located on temperature axis at $t = \frac{1}{3}$. For $D > 0$ one finds the T phase and $D < 0$, the Z phase [Fig. 1(b)].

$0.462 < K < 1$. We have a BCP in the $D > 0$ region of $D-t$ plane, as shown in Fig. 1(c). The flop line bends upward.

$0.462 > K > 0$. In this case the critical line $f_1=0$ meets a first-order phase transition line of Z phase

to paramagnetic phase [Fig. 1(d)]. The $Z \rightarrow P$ line before meeting the $T \rightarrow P$ transition line has gone through its TCP.

The determination of the flop line in all above cases is done by comparing the two free energies corresponding to the two phases of Z and T ordering. At $t=0$ the flop transition takes place when $D = 4(\sqrt{K} - K)$.

The coordinates of BCP in the $D-t$ plane for any value of $K > 0.462$ can be found from Fig. 2. In this figure $D_c(\gamma)$ and $d_c(\gamma)$ are plotted as a function of γ . Since $K = D_c/d_c$ at BCP, one should find the value of γ such that the ordinates for the two curves has a ratio equal to K . Then t_b can be found from $\gamma_b = \beta_b D_b = D_b/t_b$.

One should note the similarity of the phase diagrams in the $D-t$ plane, with those of an anisotropic antiferromagnet in a parallel external field. As in the case of an antiferromagnet, the flop line separates two phases one with xy symmetry (T phase) and the other Ising-like (Z phase). Phase diagrams similar to Fig. 1(b) (near the flop line) have been suggested by Bruce and Aharony¹⁰ for structural phase transitions in perovskites, with basically the same symmetries as mentioned above.

IV. PHASE TRANSITIONS IN A FINITE FIELD

A. $K > 0.462$

1. Field along z axis

In the presence of a magnetic field along the z axis two possible phases exist: one with moments along the field and the other with canted magnetic moments. The second-order phase transition between the two phases can be easily understood by taking $\langle S_1 \rangle$ as the order parameter and expanding the free energy as a Taylor series in powers of $\langle S_1 \rangle$. The equation for the critical line is found by setting the coefficient of the second-order term equal to zero, with the condition that the coefficient

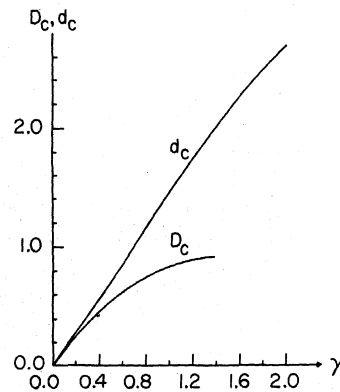


FIG. 2. Plot of D_c , Eq. (3.4), and d_c , Eq. (3.6), as functions of $\gamma = D/t$. This plot is used to obtain the BCP for $K > 0.462$.

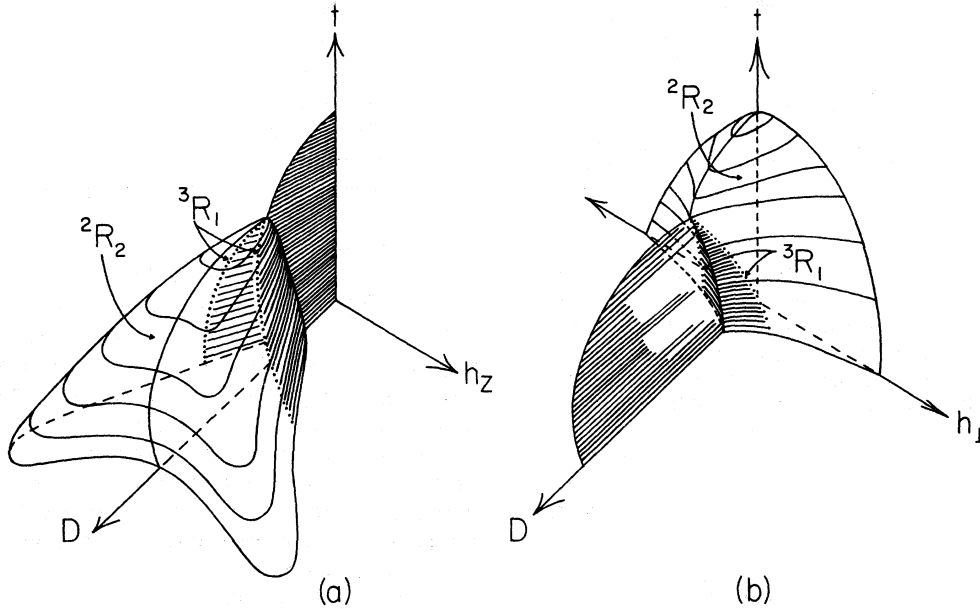


FIG. 3. Schematic phase diagrams in the (D, h_z, t) and (D, h_1, t) hyperplanes ($K > 0.462$). The hatched regions are the coexistence surfaces. 2R_2 and 3R_1 denote the two-dimensional critical surface of order 2, and the one-dimensional critical surface of order 3 (tricritical line), respectively (Ref. 12). In each phase diagram two 3R_1 surfaces meet at the BCP (4R_0).

of the fourth-order term is positive:

$$\left(\frac{1}{D-\alpha_z} + \frac{1}{2K}\right)e^{\beta\alpha_z} + \left(\frac{1}{D+\alpha_z} + \frac{1}{2K}\right)e^{-\beta\alpha_z} - \left(\frac{1}{D-\alpha_z} + \frac{1}{D+\alpha_z} - \frac{1}{2K}\right)e^{\beta D} = 0, \quad (4.1)$$

where

$$\alpha_z = 2\langle S_z \rangle_0 + h, \quad (4.2)$$

$$\langle S_z \rangle_0 = (e^{\beta\alpha_z} - e^{-\beta\alpha_z}) / (e^{\beta\alpha_z} + e^{-\beta\alpha_z} + e^{\beta D}). \quad (4.3)$$

The coefficient of the fourth-order term is rather involved and is given in Ref. 18. The numerical computation of this coefficient is straightforward. The simultaneous vanishing of the second- and fourth-order coefficients gives the tricritical point (TCP).

In discussing the phase diagrams, we shall always consider the parameter K as fixed. If then we treat the anisotropy parameter D as a field, we would have a thermodynamic field space for description of the phase diagrams consisting of the three variables D , t , and h_z (putting the ordering field $h_1=0$). Then the phase diagrams are the extension of those considered in Sec. III, to the $h_z \neq 0$ region. The (D, t, h_z) field space is necessary for understanding the nature of BCP and the geometry of phase diagrams close to it. The variation of this geometry with the transverse coupling K will provide us with the complete qualitative description of

the phase transitions.

If the anisotropy parameter D is also fixed, then we can study the phase diagram in the (h_z, t) plane. These phase diagrams are convenient for the study of TCP. Application of an ordering field h_1 will generate the wings. One should note that here the whole relevant thermodynamic field space (h_1, h_z, t) is experimentally accessible.

To discuss the phase diagrams, especially close to BCP, we consider two typical values of K , $K=0.6$ (>0.462) and $K=0.35$ (<0.462). The latter case will be discussed after the $K=0.6$ case is fully explained in both parallel and transverse fields.

The three-dimensional phase diagram in (D, t, h_z) space is sketched in Fig. 3(a). Three cross sections of this phase diagram at different temperatures of $t=0$, $t=0.65$, and $t=0.8$ are shown in Fig. 4. At $t=0$, we have a quenched moment state at $h_z=0$, if $D \geq 4K$. By increasing the external field the system undergoes a phase transition from the quenched to the canted phase (curve a). The order parameter is $\langle S_1 \rangle$. One can easily show that this transition is always of second order¹⁸ for all values of K , and the equation of this curve is given by

$$h_{c1} = [D(D-4K)]^{1/2}. \quad (4.4)$$

The line b on Fig. 4 is the locus of transition points from the canted phase to the paramagnetic phase as h_z is increased. The order parameter for this transition is again the moment $\langle S_1 \rangle$, which vanishes

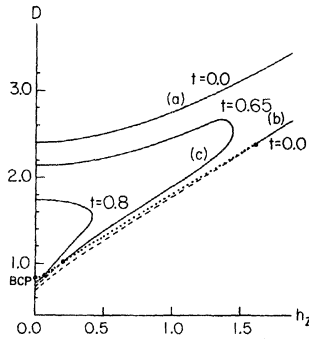


FIG. 4. (D, h_z) cross sections of Fig. 3(a) for $K=0.6$ at different temperatures. The two $t=0.0$ lines a and b meet at infinity and enclose the canted phase. Solid lines and dashed lines represent, respectively, the second-order and the first-order phase boundaries. The dotted line is the projection of the line of tricritical points in Fig. 3(a) on the (D, h_z) plane.

at the transition point if it is of the second order. The second-order part of curve b is given by

$$h_{c_2} = D + 2(K - 1). \quad (4.5)$$

The lines of first- and second-order transitions join at TCP located by

$$2K^2 + 2(D - 1)K - D = 0. \quad (4.6)$$

The two curves a and b meet at $D = h_z = \infty$. At any finite temperature the two lines join at finite D and h_z (curve c). As temperature increases the area shrinks to a point at BCP. As shown in Fig. 3, the two lines of TCP (2R_1) bounding the critical surfaces (2R_2) (notation due to Chang, Hankey, and Stanley¹²) meet each other at the BCP.

Some (h_z, t) cross sections of the phase diagram Fig. 3(a) for different D values are shown in Fig. 5. The projection of the line of TCP's is also included in these diagrams. Such (h_z, t) phase diagrams deserve a special interest: since $\langle S_1 \rangle$ is the order parameter, its conjugate h_1 can be utilized to set up a three-dimensional phase diagram in (h_1, h_z, t) space. The accessibility of the whole thermodynamic field space is a point we want to emphasize. To have a TCP in (h_z, t) plane, the parameter K should be greater than 0.462, and D should be in the following range:

$$D_K < D < \frac{2K^2 - 2K}{1 - 2K}, \quad (4.7)$$

where, D_K satisfies the equation

$$\frac{4K - D_K}{3D_K K} \ln \frac{4K + 2D_K}{4K - D_K} = 1. \quad (4.7a)$$

For $K=0.6$, D should lie in the range $0.83 < D < 2.4$ to have a TCP in an applied field h_z .

An interesting case is $K=1.0$. From Eqs. (4.4) and (4.5) one can find the corresponding curves a and b at $t=0$ while Eq. (4.6) gives the TCP at $t=0$ at $(D=0, h_z=0)$. At finite t , a similar situation prevails, i. e., the balloonlike surface in Fig. 3(a) is totally a critical surface and the two tricritical lines we had for $K < 1$ coincide with the flop line, now on the t axis.

2. Field in the basal plane

With a field applied in the transverse direction, while $h_z=0$, we have a three-dimensional phase diagram in the (D, h_1, t) field space, as given schematically in Fig. 3(b). The surface of the second-order transition can be obtained by a perturbative expansion similar to the one discussed in Ref. 18. Again we would have the free energy expanded in even powers of $\langle S_z \rangle$. Vanishing of the second-order term in the expansion gives the critical point, while the fourth-order term is positive. The equation of surface of second-order transitions thus obtained is

$$(4/z_0)(b_0 e^{-\beta\epsilon_0} + b_1 e^{-\beta\epsilon_1} + b_2 e^{-\beta\epsilon_2}) = 1, \quad (4.8)$$

where

$$b_0 = \frac{D}{h_1^2}, \quad b_1 = -\frac{\epsilon_1}{x\epsilon_2}, \quad b_2 = \frac{\epsilon_2}{x\epsilon_1}, \quad (4.9)$$

$$x = (D^2 + 4\alpha_0^2)^{1/2}, \quad (4.10)$$

$$\alpha_0 = h_1 + 2K \langle S_1 \rangle_0, \quad (4.11)$$

$$\epsilon_{1,2} = \frac{1}{2}D \mp \frac{1}{2}x, \quad \epsilon_0 = D, \quad (4.12)$$

and

$$z_0 = \sum e^{-\beta\epsilon_i}. \quad (4.13)$$

$\langle S_1 \rangle_0$ is the transverse moment when $\langle S_z \rangle = 0$ and is given by the following self-consistent equation:

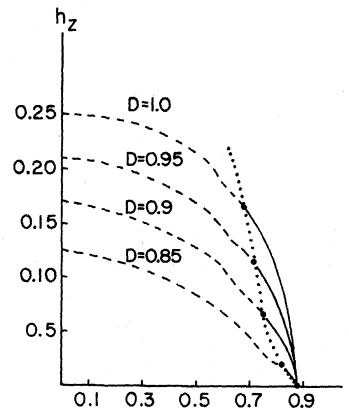


FIG. 5. (h_z, t) phase diagrams for $K=0.6$ and various values of the anisotropy D . The projection of the tricritical line in Fig. 3(a) on the (h_z, t) plane is displayed by the dotted line.

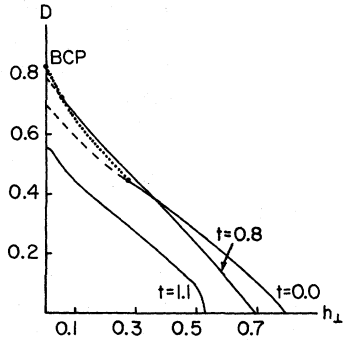


FIG. 6. (D, h_1) phase diagrams for $K=0.6$. These phase diagrams are cross sections of Fig. 3(b). For $t > 0.924$, the phase diagram consists only of a second-order line. The dotted line is the locus of the tricritical points.

$$\langle S_{\perp} \rangle_0 = \frac{4\alpha_0 \sinh(\frac{1}{2}\beta x)}{x[2 \cosh(\frac{1}{2}\beta x) + e^{-\gamma/2}]}. \quad (4.14)$$

Again the equation of the fourth-order coefficient is quite involved although its numerical calculation is straightforward.

When $D=0$ one can obtain easily the equation of the second-order line:

$$h_{\perp} = 2(1-K)\langle S_{\perp} \rangle, \quad (4.15)$$

$$\langle S_{\perp} \rangle = B_1(y), \quad (4.16)$$

$$y = 2\beta\langle S_{\perp} \rangle. \quad (4.17)$$

$B_1(y)$ is the Brillouin function.

In Fig. 3(b), the two coexistence surfaces (shaded) intersect each other at the flop line which ends up in the BCP. The two tricritical lines (3R_1) bounding the critical surfaces 2R_2 , also meet at the BCP. Figure 6 shows some constant temperature cross sections of this phase diagram (for $K=0.6$). The

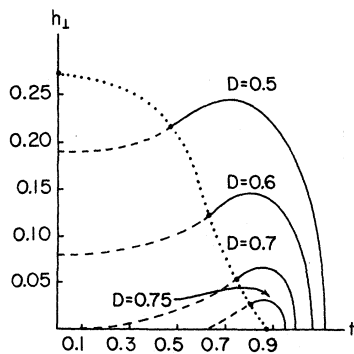


FIG. 7. (h_1, t) phase diagrams for $K=0.6$ and various values of anisotropy D . Solid lines and dashed lines represent, respectively, the second, and the first-order phase boundaries. The dotted line is the projection of the tricritical line on the (h_1, T) plane.

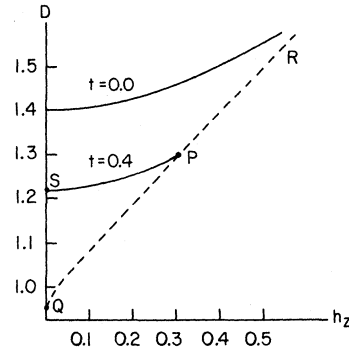


FIG. 8. (D, h_2) phase diagrams for $K=0.35$. The first-order lines (dashed) PQ and PR terminate the second-order (solid) boundary of the canted phase at point P . As t increases the canted phase region decreases.

projections of the tricritical lines in the $(D-h_1)$ plane are also shown in Fig. 6. As the temperature increases these lines get shorter, and finally vanish (at $t=0.924$). The (h_1, t) phase diagrams, Fig. 7, contain a TCP, for D within a certain range. Here again we have the possibility of observing the wing coexistence surfaces in the accessible field space of (h_1, h_2, t) . For the particular value of $K=0.6$, D should lie between 0.44 and 0.83 to have a TCP.

It should be noted that the range of values of D where a TCP can be seen on the phase diagram is somewhat wider than that given by Eq. (4.7). For example for $K=0.6$, if $0.44 < D < 2.4$, one has the possibility of getting a TCP by applying one of the two fields h_2 or h_1 .

B. $0 < K < 0.462$

In Sec. III we noted that at $\vec{H}=0$ we do not have a BCP on the $D-t$ phase diagram if $0 < K < 0.462$, Fig. 1(d). When $D > D_0 = 4(\sqrt{K} - K)$, the system initially orders in the basal plane, while it orders along z axis for $D < D_0$. For a typical value of $K=0.35$, $D_0=0.96$. When $D > D_0$ ($D < D_0$) one can apply a field along a longitudinal (transverse) direction, without it being conjugate to the proper order parameter.

A phase diagram in the $(D-h_2)$ plane at constant t for $K=0.35$ and $D > D_0$ is shown in Fig. 8; it consists, for all temperatures, of two coexistence lines QP (between the canted and the paramagnetic phases) and PR (between the states with longitudinal moments only), and a second-order transition line SP . These three lines intersect one another at point P . As temperature is raised, the point P moves down and the area of the region of canted phase decreases. This area shrinks to zero at $t=0.67$ (independent of the value K). The phase diagram exhibits no TCP for any value of K in this range.

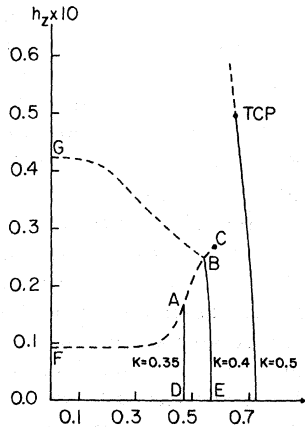


FIG. 9. (h_z, t) phase diagrams for $D=0.98$ and three different values of the transverse coupling: $K=0.35$, 0.4 , and 0.5 . For $K < 0.462$ no TCP exists but a critical end point C at $(0.27, 0.58)$.

The h_z - t phase diagrams at $D=0.98 > D_0$ are shown in Fig. 9, for several values of K . For $K=0.35$ ($K=0.4$), there exist two lines of first-order phase transitions AC (BC for $K=0.4$) and AF (BG) and a critical line AD (BE), which intersect at the point A (B). The slopes of the lines at the intersection point are different in general, although they appear to be equal in the drawing. The line AC (BC) describes a phase change between the two states with longitudinal moments only, and is in fact, a part of a cross section of the wing CXS in the Blume-Capel model (cf. Ref. 19). It is also clear from the figure that as K increases, this coexistence line shortens, and the canted phase region increases. At $K=0.462$ it completely disappears.

When $D < D_0$, the system exhibits tricriticality, only in an applied field in a transverse direction. The D - h_1 phase diagram for $K < 0.462$, Fig. 10, resembles the D - h_1 diagrams for $K > 0.462$. For $K=0.35$ the phase diagram exhibits a change in the nature of phase transition for systems with D value in the range $0.56 < D < 0.924$, and the corresponding tricritical temperature range $0 < t_t < 0.67$. Since in this range of temperature D - h_1 phase diagrams lie very close together, we have only drawn the $T=0.4$ case in Fig. 10. TCP for several values of temperature are also depicted on the diagram.

The limiting case of $K=0$ corresponds to the Blume-Capel model in a transverse field which has been discussed in detail elsewhere.¹⁷

V. CONCLUSION

We have studied an $S=1$ ferromagnetic model with both exchange and single-ion anisotropy. A summary of the main features of the model as revealed by an MFA calculation is as follows:

(i) The model characterized by the Hamiltonian (2.1) exhibits two kinds of ordering, and therefore two kinds of critical behavior are expected in zero field, depending on the magnitudes of the anisotropy parameter D and transverse coupling K . The two kinds of ordering are labeled as Z (Ising-like) and T (xy -like). They are separated by a CXS (coexistence surface), the flop line, in the D - t phase diagram.

(ii) The phase diagram in the D - t plane ($\vec{h}=0$) contains a BCP, if the transverse coupling $K > 0.462$. BCP is the terminus of the flop line CXS. As the transverse coupling is increased the BCP moves towards the temperature axis, and in the limit of isotropic exchange it lies along the t axis.

(iii) In the presence of an external magnetic field (along either the parallel or the transverse direction) there exists a TCP in the (h, t) plane, provided that K and D are within certain ranges which are by no means narrow.

(iv) In the four-dimensional field space of (D, h_1, h_2, t) , four tricritical lines approach the BCP when $0.462 < K < 1$.

At $\vec{h}=0$, the flop line is the locus of the coexistence of four ferromagnetic phases. To distinguish these phases we should apply the infinitesimal fields $\pm h_z \rightarrow 0$ and $\pm h_1 \rightarrow 0$. We designate these phases by Z^+ , Z^- , T^+ , and T^- . The signs $+$ and $-$ indicate the direction of the infinitesimal fields. In the notation of Chang, Hankey, and Stanley¹² the flop line is an 4X_1 CXS. Since a $(d+1)$ -dimensional CXS ${}^pX_{d+1}$ (p being the number of the phases coexisting) is bounded by a critical surface (CRS) of dimension d and order p , our BCP is a critical point of order 4, 4R_0 . Chang *et al.*¹² and Hankey *et al.*¹² have carried out a rather general study of the critical points of higher order. Based on an Ising model with variable interplanar interactions, they have demonstrated that a 4R_0 critical point is the intersection of several tricritical lines. A similar situ-

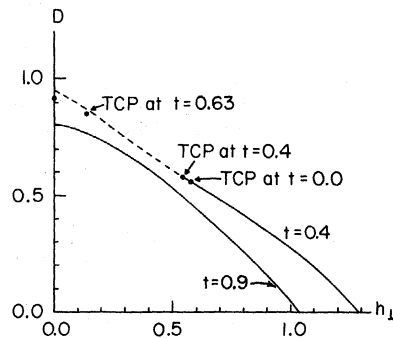


FIG. 10. (D, h_1) phase diagrams for $K=0.35$ and two values of temperature. The phase diagram resembles Fig. 6.

ation prevails at the BCP of our model.

The assumption of homogeneity near a BCP (or a 4R_0) has important consequences. In addition to the bicritical scaling laws, the tangency of the critical lines to the flop line may be of special importance. Also of interest is the competition between critical, bicritical, and tricritical behaviors in the vicinity of the BCP, which results in crossovers between these different criticalities. Hankey *et al.*,¹² based on the simultaneous validity of the scaling groups of critical points of order 2 (ordinary critical point) and 3 (tricritical point) with that of order 4, have arrived at the "double and triple scaling functions" for the singular part of the Gibbs potential, and have discussed the corresponding crossover regions. Most of the systems exhibiting bicriticality (uniaxial antiferromagnets⁵ and anisotropically stressed perovskites¹⁰) suffer from the restriction that the ordering field is either fictitious or uncontrollable in the laboratory. This

restriction delimits a complete scan of the vicinity of the BCP in all directions. The model discussed in this paper, though not suffering from this restriction, is subjected to another limitation in the study of BCP: A controlled variation of D in a real magnet, if not impossible, is rather difficult (although there are evidences that D can be varied by applying a pressure to the crystal²⁰).

Perhaps the most interesting feature of this model is the TCP behavior. Since the ordering field is experimentally accessible, the wing CXS's are wholly in the experimental field space. The range of the parameters K and D to permit a TCP in an external field is significantly large. Therefore, a search for a system with the model Hamiltonian (2.1) is highly desirable.

A study of this model in the light of the recent works by Fisher and Nelson,⁵ Nelson, Kosterlitz, and Fisher,¹⁴ and Bruce and Aharony¹⁰ will be published later.

*Supported in part by the Committee on Faculty Research Support.

†Supported in part by National Science Foundation under Grant No. GH-40174.

¹Ph. Kohnstamm, in *Handbuch der Physik*, Vol. 10, edited by H. Geiger and K. Scheel (Springer, Berlin, 1926), p. 223; I. R. Krichevskii *et al.*, *Russ. J. Phys. Chem.* **37**, 1046 (1963); G. S. Radyshevskaya *et al.*, *J. Gen. Chem. USSR* **32**, 673 (1962); see also R. B. Griffith and B. Widom, *Phys. Rev. A* **8**, 2173 (1973), and references cited therein.

²E. H. Graf, M. Lee, J. D. Reppy, *Phys. Rev. Lett.* **19**, 417 (1967); I. S. Jacobs and P. E. Lawrence, *Phys. Rev.* **164**, 866 (1967); G. Goellner and H. Meyer, *Phys. Rev. Lett.* **26**, 1534 (1971); D. P. Landau, B. E. Keen, B. Schneider, and W. P. Wolf, *Phys. Rev. B* **3**, 2310 (1971); M. Blume, V. J. Emery, and R. B. Griffith, *Phys. Rev. A* **4**, 1071 (1971).

³C. J. Gorter and T. Van Peski-Tinbergen, *Physica (Utr.)* **22**, 273 (1956).

⁴G. A. Smolenski, *Fiz. Tverd. Tela* **4**, 1095 (1962) [*Sov. Phys. - Solid State* **4**, 807 (1962)].

⁵M. E. Fisher and D. R. Nelson, *Phys. Rev. Lett.* **32**, 1350 (1974); A. Aharony and A. D. Bruce, *ibid.* **33**, 1350 (1974).

⁶Ch. Wissel, *Phys. Status Solidi B* **51**, 699 (1972), and references cited therein.

⁷H. Weitzel, *Z. Kristallogr.* **131**, 239 (1970); H. A. Obermayer, H. Dachs, and H. Schröke, *Solid State*

Commun. **12**, 779 (1973).

⁸K. S. Liu and M. E. Fisher, *J. Low. Temp. Phys.* **10**, 665 (1973).

⁹F. Wegner, *Solid State Commun.* **12**, 785 (1973).

¹⁰A. D. Bruce and A. Aharony, *Phys. Rev. B* **11**, 478 (1975).

¹¹R. Bausch, *Z. Phys.* **254**, 81 (1972).

¹²T. S. Chang, A. Hankey, H. E. Stanley, *Phys. Rev. B* **8**, 346 (1973); A. Hankey, T. S. Chang, and H. E. Stanley, *ibid.* **8**, 1178 (1973).

¹³F. Harbus, A. Hankey, H. E. Stanley, and T. S. Chang, *Phys. Rev. B* **8**, 273 (1973).

¹⁴D. Nelson, J. M. Kosterlitz, and M. E. Fisher, *Phys. Rev. Lett.* **33**, 813 (1974).

¹⁵ $n^*(d) \approx (4 + 3.176 \epsilon) / (1 + 1.294 \epsilon)$ up to order ϵ^3 ($\epsilon = 4 - d$). See Refs. 5 and 14.

¹⁶The real nature of the staggered fields in certain antiferromagnets is discussed in M. Blume, L. M. Corliss, J. M. Hastings, and E. Schiller, *Phys. Rev. Lett.* **32**, 554 (1974).

¹⁷M. R. H. Khajepour, R. A. Kromhout, and Yung-Li Wang, *J. Phys. A* **8**, 913 (1975).

¹⁸Yung-Li Wang and M. R. H. Khajepour, *Phys. Rev. B* **6**, 1778 (1972).

¹⁹M. Blume, J. V. Emery, and R. B. Griffith, *Phys. Rev. A* **4**, 1071 (1971).

²⁰D. Meier, M. Kornezos, and S. A. Friedberg, *AIP Conf. Proc.* **2**, 1316 (1974).